Research Article | Vol. 7, No. 1 | 1 Jan 2017 | OPTICAL MATERIALS EXPRESS 253

Optical Materials EXPRESS

Photonic-crystal hydrogels with a rapidly tunable stop band and high reflectivity across the visible

JIN-GYU PARK,[1] W. BENJAMIN ROGERS,[1,2] SOFIA MAGKIRIADOU,[3] TOM KODGER,[1] SHIN-HYUN KIM,[4] YOUNG-SEOK KIM,[5] AND VINOTHAN N. MANOHARAN[1,3,*]

[1]*Harvard John A. Paulson School of Engineering and Applied Sciences, Harvard University, 17 Oxford Street, Cambridge, MA 02138, USA*
[2]*Martin A. Fisher School of Physics, Brandeis University, 415 South Street, Waltham, MA 02453, USA*
[3]*Department of Physics, Harvard University, 9 Oxford Street, Cambridge, MA 02138, USA*
[4]*Department of Chemical and Biomolecular Engineering, Korea Advanced Institute of Science and Technology, Daejeon, 305-701, South Korea*
[5]*Korea Electronics Technology Institute, 68 Yatap-dong Bundang-gu, Seongnam-si, Gyeonggi-do, South Korea*
[*]*vnm@seas.harvard.edu*
http://manoharan.seas.harvard.edu

Abstract: We present a new type of hydrogel photonic crystal with a stop band that can be rapidly modulated across the entire visible spectrum. We make these materials by using a high-molecular-weight polymer to induce a depletion attraction between polystyrene-poly(N-isopropylacrylamide-co-bisacrylamide-co-acrylic acid) core-shell particles. The resulting crystals display a stop band at visible wavelengths that can be tuned with temperature at a rate of 60 nm/s, nearly three orders of magnitude faster than previous photonic-crystal hydrogels. Above a critical concentration of depleting agent, the crystals do not melt even at 40 degrees Celsius. As a result, the stop band can be modulated continuously from red (650 nm) to blue (450 nm), with nearly constant reflectivity throughout the visible spectrum. The unusual thermal stability is due to the polymer used as the depleting agent, which is too large to enter the hydrogel mesh and therefore induces a large osmotic pressure that holds the particles together. The fast response rate is due to the collective diffusion coefficient of our hydrogel shells, which is more than three orders of magnitude larger than that of conventional bulk hydrogels. Finally, the constant reflectivity from red (650 nm) to blue (450 nm) is due to the core-shell design of the particles, whose scattering is dominated by the polystyrene cores and not the hydrogel. These findings provide new insights into the design of responsive photonic crystals for display applications and tunable lasers.

OCIS codes: (160.5298) Photonic crystals; (160.0160) Materials; (160.4670) Optical materials.

References and links

1. J. H. Holtz and S. A. Asher, "Polymerized colloidal crystal hydrogel films as intelligent chemical sensing materials," Nature **389**, 829–832 (1997).
2. M. Ben-Moshe, V. L. Alexeev, and S. A. Asher, "Fast responsive crystalline colloidal array photonic crystal glucose sensors," Anal. Chem. **78**, 5149–5157 (2006).
3. Y. Kang, J. J. Walish, T. Gorishnyy, and E. L. Thomas, "Broad-wavelength-range chemically tunable block-copolymer photonic gels," Nat. Mater. **6**, 957–960 (2007).
4. T. Kanai, D. Lee, H. C. Shum, R. K. Shah, and D. A. Weitz, "Gel-immobilized colloidal crystal shell with enhanced thermal sensitivity at photonic wavelengths," Adv. Mater. **22**, 4998–5002 (2010).
5. J. Ge and Y. Yin, "Responsive photonic crystals," Angew. Chem. Int. Ed. **50**, 1492–1522 (2011).
6. K. I. MacConaghy, C. I. Geary, J. L. Kaar, and M. P. Stoykovich, "Photonic crystal kinase biosensor," J. Am. Chem. Soc. **136**, 6896–6899 (2014).
7. C. Fenzl, T. Hirsch, and O. S. Wolfbeis, "Photonic crystals for chemical sensing and biosensing," Angew. Chem. Int. Ed. **53**, 3318–3335 (2014).
8. J. M. Weissman, H. B. Sunkara, S. T. Albert, and S. A. Asher, "Thermally switchable periodicities and diffraction from mesoscopically ordered materials," Science **274**, 959 (1996).

#279983 http://dx.doi.org/10.1364/OME.7.000253
Journal © 2017 Received 2 Nov 2016; revised 10 Dec 2016; accepted 11 Dec 2016; published 22 Dec 2016

Optical Materials EXPRESS

9. X. Xu, A. V. Goponenko, and S. A. Asher, "Polymerized polyHEMA photonic crystals: pH and ethanol sensor materials," J. Am. Chem. Soc. **130**, 3113–3119 (2008).
10. M. M. Ward Muscatello, L. E. Stunja, and S. A. Asher, "Polymerized crystalline colloidal array sensing of high glucose concentrations," Anal. Chem. **81**, 4978–4986 (2009).
11. J.-T. Zhang, L. Wang, J. Luo, A. Tikhonov, N. Kornienko, and S. A. Asher, "2-D array photonic crystal sensing motif," J. Am. Chem. Soc. **133**, 9152–9155 (2011).
12. T. Tanaka and D. J. Fillmore, "Kinetics of swelling of gels," J. Chem. Phys. **70**, 1214–1218 (1979).
13. Y. Li and T. Tanaka, "Kinetics of swelling and shrinking of gels," J. Chem. Phys. **92**, 1365–1371 (1990).
14. S. Matsukawa and I. Ando, "A study of self-diffusion of molecules in polymer gel by pulsed-gradient spin-echo ^{1}H NMR," Macromolecules **29**, 7136–7140 (1996).
15. T. Tanaka, E. Sato, Y. Hirokawa, S. Hirotsu, and J. Peetermans, "Critical kinetics of volume phase transition of gels," Phys. Rev. Lett. **55**, 2455 (1985).
16. M. Andersson, A. Axelsson, and G. Zacchi, "Swelling kinetics of poly (N-isopropylacrylamide) gel," J. Control. Release **50**, 273–281 (1998).
17. J. D. Debord and L. A. Lyon, "Thermoresponsive photonic crystals," J. Phys. Chem. B **104**, 6327–6331 (2000).
18. L. A. Lyon, J. D. Debord, S. B. Debord, C. D. Jones, J. G. McGrath, and M. J. Serpe, "Microgel colloidal crystals," J. Phys. Chem. B **108**, 19099–19108 (2004).
19. M. Chen, L. Zhou, Y. Guan, and Y. Zhang, "Polymerized microgel colloidal crystals: photonic hydrogels with tunable band gaps and fast response rates," Angew. Chem. Int. Ed. **52**, 9961–9965 (2013).
20. Y. Takeoka and M. Watanabe, "Polymer gels that memorize structures of mesoscopically sized templates. Dynamic and optical nature of periodic ordered mesoporous chemical gels," Langmuir **18**, 5977–5980 (2002).
21. K. Ueno, K. Matsubara, M. Watanabe, and Y. Takeoka, "An electro- and thermochromic hydrogel as a full-color indicator," Adv. Mater. **19**, 2807–2812 (2007).
22. K. Matsubara, M. Watanabe, and Y. Takeoka, "A thermally adjustable multicolor photochromic hydrogel," Angew. Chem. Int. Ed. **46**, 1688–1692 (2007).
23. A. Perro, G. Meng, J. Fung, and V. N. Manoharan, "Design and synthesis of model transparent aqueous colloids with optimal scattering properties," Langmuir **25**, 11295–11298 (2009).
24. S. Magkiriadou, J.-G. Park, Y.-S. Kim, and V. N. Manoharan, "Disordered packings of core-shell particles with angle-independent structural colors," Opt. Mater. Express **2**, 1343–1352 (2012).
25. J.-G. Park, S.-H. Kim, S. Magkiriadou, T. M. Choi, Y.-S. Kim, and V. N. Manoharan, "Full-spectrum photonic pigments with non-iridescent structural colors through colloidal assembly," Angew. Chem. Int. Ed. **53**, 2899–2903 (2014).
26. N. Dingenouts, C. Norhausen, and M. Ballauff, "Observation of the volume transition in thermosensitive core-shell latex particles by small-angle X-ray scattering," Macromolecules **31**, 8912–8917 (1998).
27. R. Pelton, "Temperature-sensitive aqueous microgels," Adv. Colloid Interface Sci. **85**, 1–33 (2000).
28. M. J. Hore, B. Hammouda, Y. Li, and H. Cheng, "Co-nonsolvency of poly (n-isopropylacrylamide) in deuterated water/ethanol mixtures," Macromolecules **46**, 7894–7901 (2013).
29. X. S. Wu, A. S. Hoffman, and P. Yager, "Synthesis and characterization of thermally reversible macroporous poly (N-isopropylacrylamide) hydrogels," J. Polym. Sci. A Polym. Chem. **30**, 2121–2129 (1992).
30. J. Bibette, D. Roux, and B. Pouligny, "Creaming of emulsions: the role of depletion forces induced by surfactant," J. Phys. II **2**, 401–424 (1992).
31. S. Asakura and F. Oosawa, "On interaction between two bodies immersed in a solution of macromolecules," J. Chem. Phys. **22**, 1255–1256 (1954).

1. Introduction

Hydrogel photonic crystals that change their periodicity through swelling and deswelling can be used to construct chemical sensors and biosensors, diagnostic devices, and displays [1–7]. One approach to making such responsive optical materials is to embed colloidal crystals in hydrogels that can change their volume in response to a variety of stimuli [8–11]. However, the temporal response of photonic crystals prepared in this way, which is typically of order 0.01–0.05 nm/s [9, 10], is too slow for many practical applications. According to the theory of hydrogel swelling developed by Tanaka and Fillmore, the motion of the gel network obeys a diffusion equation [12–14]: The swelling time is proportional to the square of the size of the gel and inversely proportional to its collective diffusion coefficient. This description of swelling suggests two ways to improve the response rate of hydrogel-based photonic crystals: reduce the size of the gel, or increase its collective diffusion coefficient [15, 16].

Many approaches have followed the first path—reducing the size of the gel—in an attempt to increase the response rate of photonic-crystal hydrogels. One approach is to use microgel particles

Optical Materials EXPRESS

with diameters of a few hundred nanometers to make the photonic crystal. While the microgel particles themselves respond rapidly to changes in temperature, microgel-based colloidal crystals tend to melt as they shrink, as there is no force holding the crystals together [17, 18]. To circumvent this limitation, Chen and coworkers developed a technique to interlock the microgel particles together by chemically crosslinking their surfaces to one another [19]. Another approach to reducing the characteristic length is to embed nanoscopic cavities into the microgel matrix, for instance by infiltration and subsequent removal of a colloidal crystal template [20–22]. In these so called 'inverse opal' structures, the characteristic gel size is related to the distance between the cavities, as opposed to the dimensions of the bulk gel itself. In both approaches—interlocking microgel particles and fabricating inverse structures—the response rate is indeed shown to be faster than that of homogeneous bulk hydrogels; the stop band can be modulated at rates of roughly 0.1 nm/s [19–22]. However, the reflectivity of these porous photonic hydrogels changes dramatically as the stop band is modulated [19–22]. Furthermore, their response rates are still too low to be useful for reflective displays and other applications.

Here we combine both approaches—reducing the characteristic size of the gel and increasing its collective diffusion coefficient—to make a second large leap in response rate, while also maintaining stability and constant reflectivity as the stop band is modulated. To accomplish these goals, we use core-shell particles with polystyrene (PS) cores and poly(N-isopropylacrylamide-co-bisacrylamide-co-acrylic acid, pNiPAm-BIS-AAc) shells, and assemble them into crystals using the depletion attraction. The core-shell geometry allows us to decouple scattering from the degree of swelling, thus ensuring high reflectivity at all wavelengths: The polystyrene core controls the scattering, while the thickness of the hydrogel shell controls the interparticle spacing [23–25]. We show that the sparse hydrogel shells around the polystyrene cores have a high collective diffusion coefficient, which enables them to swell and deswell rapidly. When mixed with an aqueous suspension of high-molecular-weight, non-adsorbing polyacrylamide (PAm, Mw 5,000,000–6,000,000), the core-shell nanoparticles self-assemble into colloidal crystals. We choose a large enough concentration of PAm so that the crystals do not melt even at 40°C, well above the volume phase transition temperature of pNiPAm-BIS-AAc. Through the integration of these three components—strongly scattering cores, rapidly responding shells, and large, concentrated depleting agents—we create hydrogel photonic crystals whose stop band can be modulated from 650 nm to 450 nm at about 60 nm/sec, nearly three orders of magnitude faster than the response rates of 0.1 nm/sec found for the hydrogels in References [19–22].

2. Results and discussion

We synthesize our core-shell particles by coating the surface of PS nanoparticles (d_{PS} = 156 nm) with a poly(NiPAm-BIS-AAc) shell using seeded emulsion polymerization [23–25]. During seed preparation, we incorporate 5.0 wt% NiPAm into the styrene monomer to make a random copolymer of poly(styrene-co-NiPAm). Doing so makes the surface of the nanoparticles NiPAm-rich, which allows us to grow a shell of PNIPAm-BIS-AAc through chain transfer during seeded polymerization [26]. The ratio of seed to monomer is chosen such that the total diameter is roughly half the wavelength of red light ($d_{\text{core-shell}}$ = 335 ± 8 nm) in the presence of 50 mM NaCl (Fig. 1(a)).

The resulting core-shell nanoparticles display a large and continuous change in volume with changing temperature. The total diameter of the core-shell nanoparticles varies from 335 nm at 20°C to 195 nm at 50°C (Fig. 1(b)). This behavior is consistent with the thermal response of poly(NiPAm-BIS-AAc) microgel particles [27]: The temperature range, shape of the response curve, and inflection point are roughly the same for the two systems. Since the diameter of the polystyrene core is independent of temperature, the total change in diameter of our core-shell microparticles is due to the change in volume of our poly(NiPAm-BIS-AAc) shell [26].

When dispersed in an aqueous solution of high-molecular-weight, non-adsorbing PAm, the

Optical Materials EXPRESS

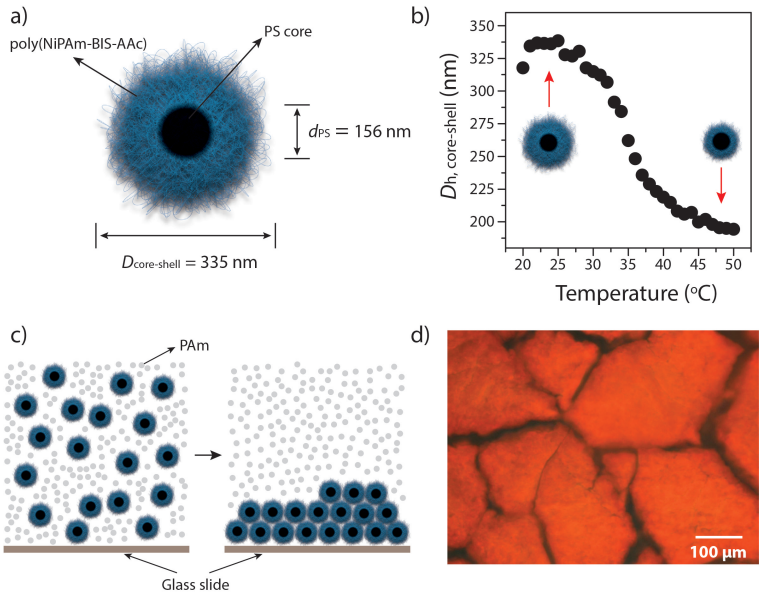

Fig. 1. Polystyrene/poly(N-isopropylacrylamide-co-bisacrylamide-co-acrylic acid, PS/PNiPAm-BIS-AAc) core-shell nanoparticles self-assemble into photonic crystals through a depletion attraction. a) Schematic of the core-shell particle. b) The hydrodynamic diameter of the core-shell particles as a function of temperature in aqueous suspension containing 50 mM NaCl. c) Self-assembly of colloidal crystals is driven by a depletion attraction induced by the presence of non-adsorbing polymer (gray dots). d) An optical micrograph of the photonic crystals formed on a glass substrate shows highly uniform structural colors.

core-shell nanoparticles spontaneously self-assemble into colloidal crystals, as illustrated in Fig. 1(c). The crystals are roughly one hundred particles thick and contain grain boundaries that separate large domains several tens of micrometers wide, as shown in the optical micrograph in Fig. 1(d). The reflected colors of the various domains are the same, indicating that the domains likely grow from crystallites that independently and heterogeneously nucleate on the glass with their (111) planes parallel to the substrate.

The stop band of these photonic crystals can be modulated across the entire visible spectrum by adjusting the temperature. When we heat the samples from 20°C to 40°C, we find that the diffraction peak blue-shifts continuously from 650 nm to 440 nm (Fig. 2(a)). A comparison of the peak position (λ_{max}) between heating and cooling shows that the shift is reversible with little hysteresis (Fig. 2(b)).

Bright-field optical micrographs (Fig. 2(c)) show that all the domains have the same color at a given temperature. As the temperature increases, the crystals shrink but retain their shape. Therefore, the grain boundaries grow larger. Upon cooling, the crystals return reversibly to the same size and color (see Fig. 5 in Appendix).

These observations suggest that each domain shrinks and grows isotropically with temperature. This isotropic shrinkage is enabled by the depletion attraction, which holds the particles together as they shrink and binds the domains to the substrate. Because there is no tangential force between the crystals and the substrate, they can grow and shrink isotropically without strain.

The intensity and width of the measured reflectance peak remain almost constant over the full range of temperatures. By comparison, photonic crystals made of pure hydrogel particles show reflectance peaks that fall dramatically with decreasing temperature [19–22]. We attribute

Optical Materials EXPRESS

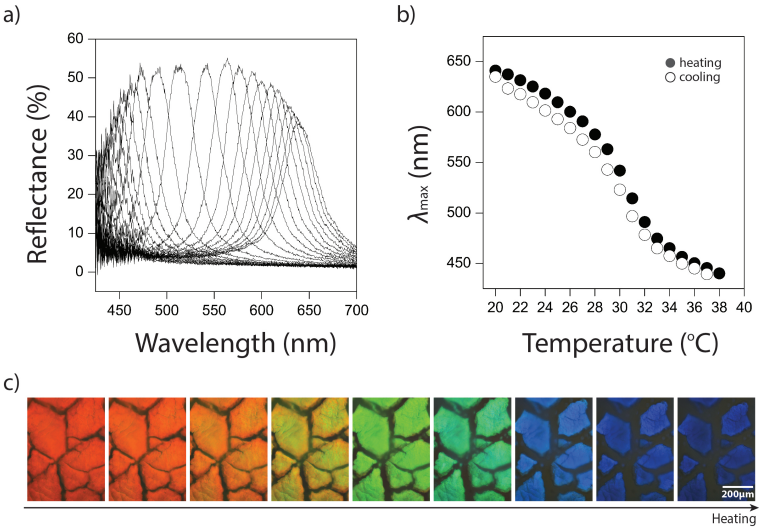

Fig. 2. PS/PNiPAm-BIS-AAc hydrogel photonic crystals display a continuous shift in the position of their stop band without melting. a) Reflectance spectra of photonic crystals taken during step-wise heating from 20°C to 40°C with a step size of 1°C. b) Peak position ($\lambda_{\max}$) as a function of temperature during heating (black circles) and cooling (white circles). We equilibrate the samples for 2 min at each temperature before measuring the spectrum. c) A series of optical micrographs of the photonic crystals taken during heating shows the uniform change in structural color upon heating.

the near-constant and high reflectivity of our samples to the polystyrene cores. In crystals made of pure microgel particles, the reflected intensity is controlled by scattering from the particles themselves. This scattering weakens as the particles swell and their effective refractive index decreases. In contrast, scattering from our core-shell particles is dominated by the polystyrene cores [23–25]. Because the refractive index and particle size of the polystyrene cores are independent of temperature, the reflected intensity of our photonic crystals remains largely constant across the visible spectrum.

The most remarkable feature of our photonic crystals is the rapid response of their stop band to changes in temperature. We measure the rate of change of the reflectance peak upon rapid heating and cooling of the samples. When the crystals are heated from 20°C to 40°C at a rate of about 2°C/sec, the peak of the stop band shifts from roughly 650 nm to 450 nm within seconds (Fig. 3(a,c)). By fitting an exponential decay of the form $\lambda_{\max} = (\lambda_2 - \lambda_1)\exp(-t/\tau) + \lambda_1$ to the peak position as a function of time, we infer that the characteristic time τ of the crystal is about 3 seconds. Therefore, the response rate, defined here as $(\lambda_2 - \lambda_1)/\tau$, is found to be about 60 nm/sec for our self-assembled photonic crystals, nearly three orders of magnitude faster than that of other photonic-crystal hydrogels [8–11, 19]. We observe a similar time constant of 7.5 seconds on cooling (Fig. 3(b,c)). In fact, the actual response is likely to be even faster than what we have measured, since there is some time required for heat to diffuse into and out of the sample.

We attribute this rapid response to the large collective diffusion coefficient of our hydrogel shell. We estimate the collective diffusion coefficient of the microgels by measuring the swelling of a macroscopic hydrogel that is polymerized under the same conditions and that has the same composition as our hydrogel shell. Specifically, we measure the radius of a centimeter-sized cylindrical hydrogel as a function of time following a sudden temperature change from 25°C to 45°C (see Fig. 6 in Appendix). From this data, we extract the characteristic time of deswelling

Optical Materials EXPRESS

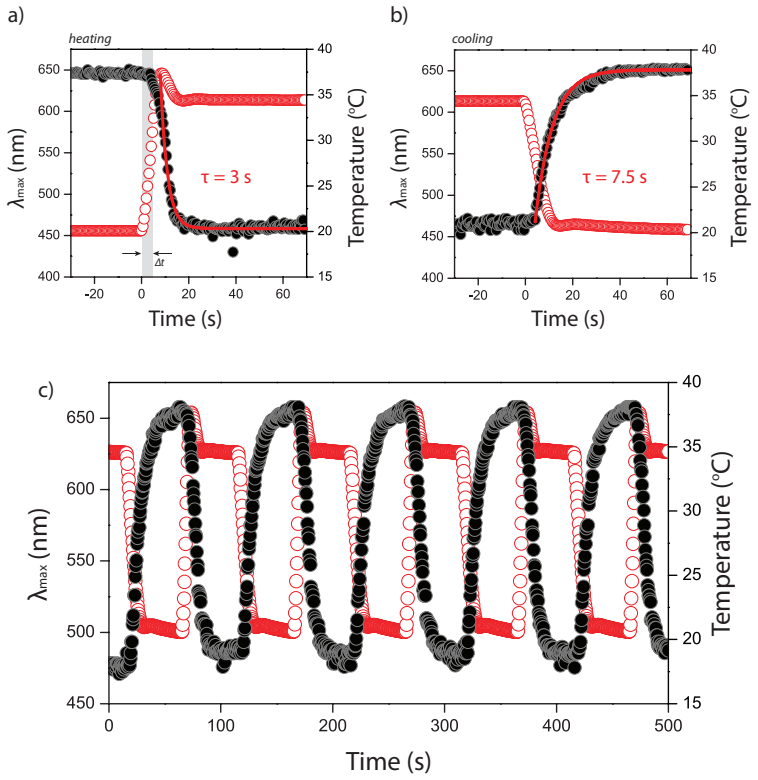

Fig. 3. PS/PNiPAm-BIS-AAc photonic crystals respond quickly to changes in temperature. a, b) Peak wavelength λ_{max} (black circles) and temperature (red circles) as a function of time during a) heating and b) cooling. After a few-second delay between the photonic-crystal response and the temperature change, Δt, the stop-band position shifts across the entire visible range with a time constant of 3 sec (heating) or 7.5 sec (cooling). c) The stop-band position λ_{max} as a function of temperature during cyclic swelling and deswelling of the crystals. The temperature is monitored by a thermistor, which is embedded in a dab of thermal paste confined between the sample and heating surface.

and calculate the collective diffusion coefficient from the time constant and the initial radius of the cylindrical gel. The value that we find, $D = 8.0 \times 10^{-3}$ cm^{2}s^{-1}, is more than three orders of magnitude larger than bulk PNIPAm hydrogels [8–13, 13, 14].

We hypothesize that the large collective diffusion coefficient is due to macropores in our hydrogel shell, which result from synthesizing them within the two-phase region of the polymer-water phase diagram. Our method of polymerizing the gel shell within the two-phase region is different from other methods used to fabricate hydrogel-based photonic crystals, which typically use organic solvents, such as ethanol, and thus take place within the one-phase region of the phase diagram [21, 22, 28]. Reports studying the effect of the polymerization conditions on microgel structure have shown that microgels made from the same components, but which differ in whether they are polymerized above or below their lower critical solution temperature (LCST), can have vastly different microstructures and response kinetics [29]. Microgels prepared above their LCST have larger pore volumes, larger average pore sizes, and display swelling/deswelling kinetics more than an order of magnitude faster than conventional hydrogels having the same composition, but which were synthesized below the LCST [29].

The non-absorbing polymer plays a crucial role in preventing the photonic crystals from

Optical Materials EXPRESS

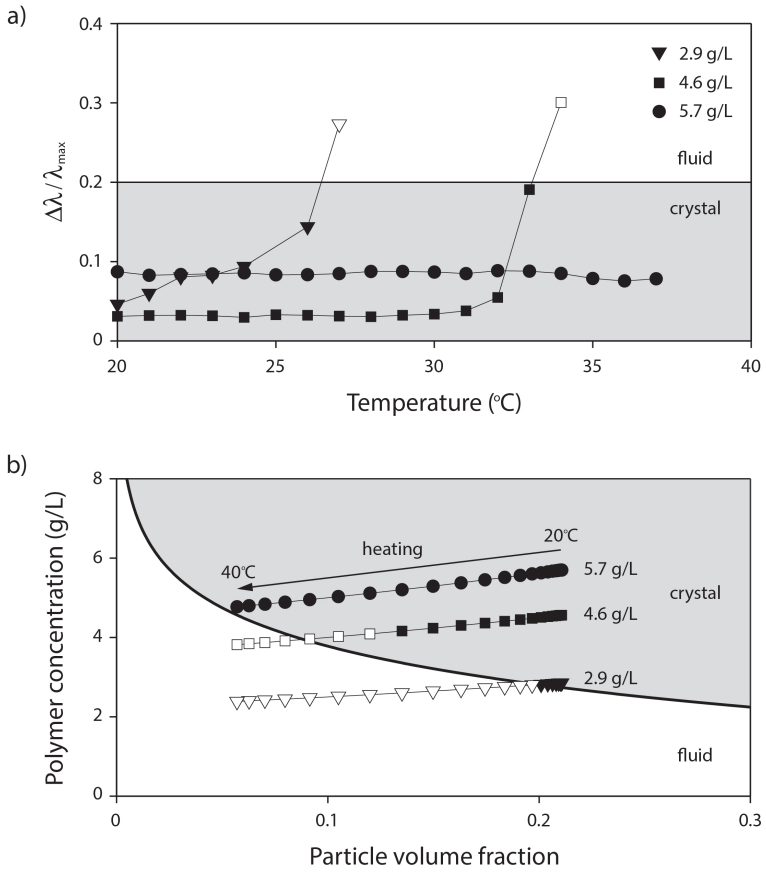

Fig. 4. The concentration of non-adsorbing polymer is critical to the stability of self-assembled photonic crystals. a) Normalized full-width at half maximum, $\Delta\lambda/\lambda_{max}$, of colloidal crystals prepared with different polymer concentrations as a function of temperature: 2.9 g/L (triangles), 4.6 g/L (squares), and 5.7 g/L (circles). We consider the crystals to be melted when $\Delta\lambda/\lambda_{max}$ exceeds 0.2. b) Equilibrium phase diagram in polymer concentration-colloid volume fraction phase space. The phase boundary is computed according to methods in Ref. [30]. The effective size of the polymer depletant is taken to be 62.5 nm, consistent with dynamic light scattering measurements. Lumped contributions due to solid entropy and van der Waals energy are treated as a free parameter, which is constrained by our data at three different polymer concentrations. Points show experimental particle volume fractions for the experimental conditions in a). Open symbols indicate the observed fluid phase, whereas filled symbols indicate the observed crystal phase.

melting; without suppressing the melting transition, we would not be able to tune the reflection peak across the entire visible spectrum. To explore the effect of the polymer concentration, we prepare samples at three different PAm concentrations: 2.9 g/L, 4.6 g/L, and 5.7 g/L. In all cases, the resulting crystals display narrow Bragg peaks ($\Delta\lambda/\lambda_{max} < 0.1$) at 20°C, as shown in Fig. 4(a). When heated, the sample prepared at 2.9 g/L shows a rapid increase in $\Delta\lambda/\lambda_{max}$ from 0.07 to 0.12, suggesting the onset of a melting transition. Above 26°C, the Bragg peak nearly disappears, and the crystal melts. In the sample prepared at 4.6 g/L, $\Delta\lambda/\lambda_{max}$ stays almost constant until the sample reaches 33°C, at which point $\Delta\lambda/\lambda_{max}$ rapidly increases, and the sample melts. At high enough polymer concentration (5.7 g/L), however, the width of the peak $\Delta\lambda/\lambda_{max}$ remains almost constant throughout the entire temperature range from 20–

Optical Materials EXPRESS

40°C, showing that the crystalline order remains intact even above the volume phase transition temperature.

To understand the stability, we calculate the phase diagram of the particles using the Asakura-Oosawa potential to model the depletion interaction [31]. We approximate the free energy of the crystal using the Einstein model and that of the fluid using the ideal gas approximation [30]. As seen in Fig. 4(b), the high polymer concentration (5.7 g/L) ensures that the sample remains within the crystalline region of the phase diagram even as the particle volume fraction decreases from 0.22 to 0.04 (black circles in Fig. 4(b)). In the case where polymer volume fraction is low, however, the system can cross the phase boundary from solid to fluid: the crystal melts at a particle volume fraction of 0.2 for 2.9 g/L (inverse triangle) and 0.12 for 4.6 g/L (square).

3. Conclusions

In summary, we have demonstrated a new type of hydrogel photonic crystal whose stop band can be rapidly modulated throughout the visible spectrum with nearly constant reflectivity. The core-shell structure of the particles and the depletion interaction enable response rates as fast as 60 nm/s, high and constant reflectivity, and stability throughout the entire visible range. The experiments we present here are the first to simultaneously reduce the characteristic length scale in the system and increase the collective diffusion coefficient of the gel. We anticipate this new two-pronged approach will be important to the continued development of responsive photonic crystals. We are currently exploring these materials as a platform for making dynamically tunable organic lasers. There are many other potential applications. For example, one could engineer crystals that respond quickly to other stimuli by introducing different functional groups in the responsive shell layer. It should also be possible to make tunable plasmonic-photonic materials with an even wider range of modulation including the visible and ultraviolet by embedding metallic nanoparticles in the shell. More generally, our approach of assembling responsive nanoparticles into photonic crystals through depletion forces provides a simple platform for fabricating dynamically tunable optical materials.

4. Materials and methods

4.1. Synthesis and characterization of core-shell particles

PS/PNiPAm hydrogel nanoparticles are fabricated by a two-step emulsion polymerization process using materials as received. In the first step, 380 mg of sodium lauryl sulfate (SLS, 99%, Aldrich) and 3.75 g of N-isopropylacrylamide (NiPAm, 97%, Aldrich) are dissolved in 230 mL of deionized (DI) water in a 500 mL three-necked round-bottom flask equipped with a reflux condenser, a nitrogen inlet, and a mechanical stirrer. Next, 78.38 mL of styrene (99%, Aldrich) are added under vigorous stirring. After heating the mixture to 80°C, 180 mg of potassium persulfate (KPS, 99%, Aldrich) dissolved in 7.5 mL of DI water are added to the reactor, and the reaction proceeds for 8 hours. The resulting PS nanoparticles are washed by dialysis against deionized water for five days. In the second step, 483 mg NiPAm, 12.0 mg N,N'-methylenebis-acrylamide (MBA, molecular biology grade, Promega), 5.0 mg of acrylic acid (AAc, 99%, Sigma), and 21 mL of the PS core suspension (5.0%, w/w) are mixed in a 40 mL glass vial. 19.0 mg of potassium persulfate dissolved in 660 mg of water are added into the vial. After mixing, we polymerize the mixture by tumbling the vial in a water bath for 3 hr at 80°C. The hydrodynamic radius of the PS core particles is 75 ± 3 nm, as measured by dynamic light scattering (DLS, ALV SP-125) with a 532 nm Verdi laser (Coherent). The hydrodynamic radius of the PS/PNiPAm core-shell colloidal particles is measured with a Malvern Nanosizer using the temperature scan mode (0.5°C/min).

Optical Materials EXPRESS

4.2. Synthesis of bulk hydrogels

Gels are synthesized by dissolving 207 mg of NiPAm, 5.4 mg of MBA, 2.1 mg of AAc, and 8 mg of KPS in 3 mL of methanol/water mixture (8/5, v/v) in a 5 mL glass vial. The precursor solution is then degassed by bubbling nitrogen gas for an hour. Next, we perform the polymerization at 65°C for 12 hr in a convection oven and then replace the solvent with DI water through dialysis over the course of a week.

4.3. Fabrication of photonic crystals

Colloidal crystals are prepared using the depletion attraction by mixing 180 μL of aqueous suspensions of PS/PNiPAm core-shell particles, 180 μL of 1.0% (w/w) aqueous PAm solution (Mw 5,000,000–6,000,000, Polyscience), and 40 μL of 0.5 M sodium chloride (NaCl). The mixture is then injected into a glass chamber made from a coverslip and a microscope slide (1.2 cm $\times$ 1.2 cm $\times$ 0.015 cm). We prevent water from evaporating by sealing the chamber with epoxy.

4.4. Characterization of photonic crystals

We control the temperature of the sample with a thermoelectric cooler (TE Technology, Inc.) that is bonded directly to the sample by silicone vacuum grease. The thermoelectric cooler is mounted to a heat sink by thermally conductive tape and driven by a high-performance digital temperature controller (Thorlabs). The sample temperature is monitored by a thermistor, which is potted in a dab of thermal paste confined between the sample and cooler surface. For static measurements of the temperature-dependent reflection spectra, the sample is equilibrated at each temperature point for roughly 2 min before data is acquired. Dynamic measurements are controlled by in-house software written in Python. Optical micrographs of the photonic crystals are taken in reflection mode on an upright optical microscope (Nikon, ECLIPSE LV100) using a 50x objective (Nikon, LU Plan Fluor, NA = 0.8) and a digital camera (Nikon DS-5Mc). We adjust the color balance in these images by normalizing to a white reflection standard (Labsphere SRS-99-010). We quantify the stop band of our photonic crystals by measuring their reflectance spectra using a fiber optic spectrometer (Ocean Optics Inc., HR2000+) attached to an optical microscope (Nikon, ECLIPSE LV100) via a 600 μm broadband optical fiber (Ocean Optics Inc., QP600-2-UV/VIS) positioned at the image plane. We use the same objective to measure the spectrum, and reflection from a mirror to normalize the measurements.

4.5. Characterization of bulk hydrogels

To estimate the collective diffusion coefficient of our hydrogel network, we monitor the diameter of a macroscopic, cylindrical gel as a function of time. We heat the hydrogel by immersing a 4 ml vial containing the bulk hydrogel suspended in water in a 1 liter water bath, which is heated to 45°C and constantly stirred by a magnetic stir bar. Images of the hydrogel are collected with a digital camera over the course of four minutes and analyzed using ImageJ. A similar procedure is performed to measure the swelling rate on cooling, but in this case the 4 ml vial containing the hydrogel is immersed in a 1 liter water bath held at 22°C.

Optical Materials EXPRESS

Appendix

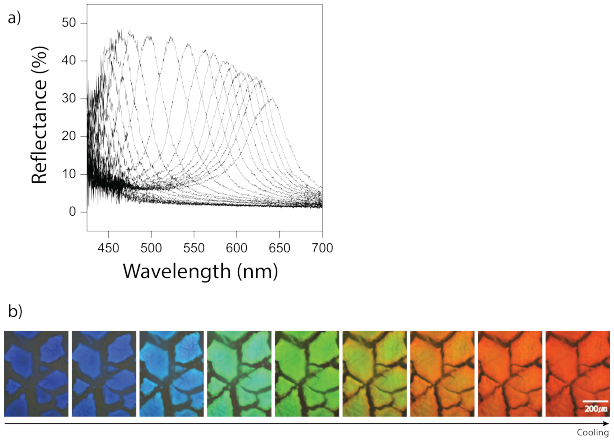

Fig. 5. a) Reflectance spectra of photonic crystals taken during step-wise cooling from 40°C to 20°C with a step size of −1°C. b) A series of optical micrographs of the photonic crystals taken during cooling.

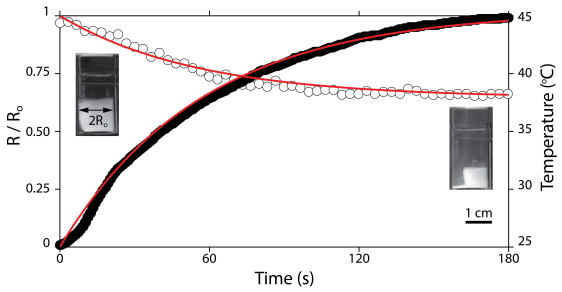

Fig. 6. The volume of a macroscopic hydrogel of poly(NiPAm-co-BIS-AAc) decreases rapidly with increasing temperature inside a glass vial (photos). Open circles show the normalized radius R/R_0 of the gel cylinder as a function of time, where R_0 is the initial radius; closed circles show the temperature as a function of time. Red curves show exponential fits.

Funding

National Science Foundation (NSF) (DMR-1420570, 1541959); Ministry of Trade, Industry, and Energy of Korea (Sunjin-2010-002); Xerox University Affairs Committee

Optical Materials EXPRESS

Acknowledgments

We thank Prof. Gi-Ra Yi from Sungkyunkwan University for helpful discussions. This work was performed in part at the Center for Nanoscale Systems (CNS) at Harvard University.